



# 1 **Influence of climate variability, fire and phosphorus limitation on the** 2 **vegetation structure and dynamics in the Amazon-Cerrado border**

3  
4 Emily Ane Dionizio da Silva<sup>1</sup>, Marcos Heil Costa<sup>1</sup>, Andrea Almeida Castanho<sup>2</sup>, Gabrielle Ferreira Pires<sup>1</sup>,  
5 Beatriz Schwantes Marimon<sup>3</sup>, Ben Hur Marimon-Junior<sup>3</sup>, Eddie Lenza<sup>3</sup>, Fernando Martins Pimenta<sup>1</sup>

6  
7 <sup>1</sup>Departamento de Engenharia Agrícola, Universidade Federal de Viçosa (UFV), Viçosa, MG, Brazil

8 <sup>2</sup>The Woods Hole Research Center, 149 Woods Hole Rd., Falmouth, MA 02540, USA

9 <sup>3</sup>Universidade do Estado de Mato Grosso, Campus de Nova Xavantina,

10 Nova Xavantina, MT, Brazil

11  
12 *Correspondence to:* Emily Ane D. da Silva (emilyy.ane@gmail.com)

## 13 **Abstract**

14 Climate, fire and soil nutritional limitation are important elements that affect the vegetation  
15 dynamics in areas of forest-savanna transition. In this paper, we use the dynamic vegetation model  
16 INLAND to evaluate the influence of climate variability, fire and phosphorus limitation on the Amazon-  
17 Cerrado transitional vegetation structure and dynamics. We assess how each element affects the net  
18 primary production, leaf area index and biomass and compare the simulations of aboveground biomass  
19 to observed biomass map. We used two climate datasets - the 1960-1990 average seasonal climate and  
20 the 1948 to 2008 interannual climate variability, two regional datasets of total soil P content in soil, based  
21 on regional (field measurements) and global data and the INLAND fire module. Our results show that  
22 climate interannual variability, phosphorus limitation and fire occurrence gradually improve simulated  
23 vegetation types and these effects are not homogeneous along the latitudinal/longitudinal gradient  
24 showing a synergistic effect among them. In terms of magnitude, the effect of fire is stronger, and is the  
25 main driver of vegetation changes along the transition. The nutritional limitation, in turn, is stronger than



26 the effect of climate variability acting on the transitional ecosystems dynamics. Overall, INLAND  
27 typically simulates more than 80% of the biomass variability in the transition zone. However, in many  
28 places, the biomass is clearly not well simulated indicating that important soil and physiological factors  
29 in the Amazon-Cerrado border, such as lithology and water table depth, carbon allocation strategies and  
30 mortality rates, still need to be included in the model.



## 31 **1 Introduction**

32           The Amazon and Cerrado are the two largest and most important phytogeographical domains in  
33 South America. The Amazon forest has been globally recognized and distinguished not only for its  
34 exuberance in diversity and species richness, but also for playing an important role in the global climate  
35 by regulating water (Bonan, 2008; Pires and Costa, 2013) and heat fluxes (Shukla et al., 1990; Rocha et  
36 al., 2004; Roy et al., 2002). The Cerrado is recognized worldwide for being the richest savanna in the  
37 world (Myers et al., 2000; Klink and Machado, 2005). It is characterized by different physiognomies,  
38 ranging from sparse physiognomies to dense woodland formations, and the latter are commonly mixed  
39 with Amazon rainforest forming transitional areas. The Amazon-Cerrado transition extends for 6270 km  
40 from northeast to southwest in Brazil, and the ecotonal vegetation around this transition is a mix of the  
41 characteristics of the tropical forest and the savanna (Torello-Raventos et al., 2013).

42           Gradients of seasonal rainfall and water deficit, fire occurrence, herbivory and low fertility of the  
43 soil have been reported as the main factors that characterize the transition between forest and savanna  
44 globally (Lehmann et al., 2011; Hoffman et al., 2012; Murphy and Bowman, 2012). However, few studies  
45 have evaluated the individual and combined effects of these factors on Brazilian ecosystems ecotones  
46 (Marimon-Junior and Haridasan, 2005; Elias et al., 2013; Vourtilis et al., 2013).

47           It is challenging to assess the degree of interaction among these various environmental factors in  
48 the transitional region and to infer how each one influences the distribution of the regional vegetation. In  
49 this case, Dynamic Global Vegetation Models (DGVMs) can be powerful tools to isolate the influences  
50 of climate, fire and nutrients, therefore helping to understand their large-scale effects on vegetation  
51 (House et al., 2003; Favier et al., 2004; Hirota et al., 2010; Hoffman et al., 2012).



52 Previous modelling studies indicate that the Amazon rainforest could experience changes in  
53 rainfall patterns which would either transform the forest into an ecosystem with more sparse vegetation –  
54 similar to a savanna, what has been called as the "savannization of the Amazon" (Shukla et al., 1990; Cox  
55 et al., 2000; Oyama and Nobre, 2003; Betts et al., 2004; Cox et al., 2004; Salazar et al., 2007) - or to a  
56 seasonal forest (Malhi et al., 2009; Pereira et al., 2012; Pires and Costa, 2013). These studies had great  
57 importance to the improvement of terrestrial biosphere modeling, but they neglect two important  
58 processes in tropical ecosystem dynamics: fire occurrence and nutrient limitation.

59 In tropical ecosystems, fire plays an important ecological role and influences the productivity, the  
60 biogeochemical cycles and the dynamics in the transitional biomes, not only by changing the phenology  
61 and physiology of plants, but also by modifying the competition among trees and lower canopy plants  
62 such as grasses, shrubs and lianas. Fire occurrence, depending on its frequency and intensity, may increase  
63 the mortality of trees and transform an undisturbed forest into a disturbed and flammable one (House et  
64 al., 2003; Hirota et al., 2010; Hoffmann et al., 2012). Fires also affect the dynamics of nutrients in the  
65 savanna ecosystem, changing mainly the N:P relationship and phosphorus availability in the soil (Nardoto  
66 et al. 2006).

67 Studies suggest that phosphorus is the main limiting nutrient within tropical forests (Malhi et al.,  
68 2009; Mercado et al., 2011; Quesada et al., 2012) unlike the temperate forests. Phosphorus is a nutrient  
69 that is easily adsorbed by soil due to the large amount of iron and aluminum oxides in the Amazon and  
70 Cerrado acidic and strongly weathered soils (Dajoz, 2005; Goedert, 1986). In the tropics, the warm and  
71 wet climate favors the high biological activity in the soil and the litter decomposition, not limiting the  
72 nitrogen for plant fixation. In Cerrado, higher soil fertility is related to regions with greater woody plants



73 abundance and less grass cover, similarly to the features found in the Amazon rainforest (Moreno et al.,  
74 2008; Vourtilis et al., 2013; Veenendaal et al., 2015). However, the phosphorus limitation is often  
75 neglected by DGVMs that usually assumes unlimited phosphorus availability and consider nitrogen as  
76 the main limiting nutrient. As it affects the dynamics between trees and grasses, the transition vegetation  
77 between ecosystems may be misrepresented in such models.

78 In principle, in transitional forests, where the climate is intermediate between wet and seasonally  
79 dry, the structure and phenology is heterogeneous among individuals which makes difficult its  
80 representation. The Amazon-Cerrado border is the result of the expansion and contraction of the Cerrado  
81 into the forest (see Marimon et al., 2006; Morandi et al., 2016), especially in the Mato Grosso state, where  
82 extreme events, such as intense droughts, influence the vegetation dynamics (Marimon et al., 2014) and  
83 the nutrient (Oliveira et al., *in press*) and carbon cycling (Valadão et al., 2016).

84 Currently, no model has demonstrated to be able to accurately simulate the vegetation transition  
85 between Amazon and Cerrado. A better understanding of the main drivers that determine the distribution  
86 of different vegetation physiognomies in the region is crucial for more reliable simulations of the  
87 transitional tropical ecosystems in future climate scenarios.

88 In this paper, we use the dynamic vegetation model INLAND (Integrated Model of Land Surface  
89 Processes) to evaluate the influence of climate variability, fire occurrence and phosphorus limitation in  
90 the Amazon-Cerrado transitional vegetation dynamics and structure. We assess how each element affects  
91 the net primary production (NPP), leaf area index (LAI) and biomass and compare the simulations of  
92 aboveground biomass (AGB) to an observed biomass map. The results presented here are important to



93 build models that accurately represent the actual transition vegetation, and show the need to include the  
94 spatial variability of eco-physiological parameters in these areas.

## 95 **2 Materials and methods**

### 96 **2.1 Study Area**

97 The present study focuses on the Amazon-Cerrado transition (Figure 1). We use the official  
98 delimitation of the Brazilian biomes proposed by IBGE (2004), and define five transects along the  
99 transition border. Transects 1 to 4 were established considering approximately 330 km into the Amazon  
100 and 330 km into the Cerrado domain, while Transect 5 is 880 km long on the southern Amazon-Cerrado  
101 border. The transects are located as follows: Transect 1 (T1, 43°- 49°W; 5°- 7°S), Transect 2 (T2, 46°-  
102 51° W; 7°-9S), Transect 3 (T3, 48°-54° W; 9°-11° S), Transect 4 (T4, 49° - 55° W; 11°-13° S), and  
103 Transect 5 (T5, 53° - 61° W; 13°-15° S) (Figure 1).

### 104 **2.2 Description of the INLAND Surface Model**

105 The Integrated Model of Land Surface Processes (INLAND) is the land-surface component of the  
106 Brazilian Earth System Model (BESM). INLAND is based on the IBIS model (Integrated Biosphere  
107 Simulator, Foley et al., 1996) which considers changes in the composition and structure of vegetation in  
108 response to the environment and incorporates important aspects of biosphere-atmosphere interactions.  
109 The model simulates the exchanges of energy, water, carbon and momentum between soil-vegetation-  
110 atmosphere. These processes are organized in a hierarchical framework and operate at different time steps,  
111 ranging from 60 minutes to 1 year, coupling ecological, biophysical and physiological processes  
112 (Kucharik et al., 2000). The vegetation structure is represented by two layers: upper and lower canopies,



113 and the composition is represented by 12 plant functional types (PFTs) (e.g., tropical broadleaf evergreen  
114 trees or C4 grasses).

115 These PFTs can coexist within a grid cell and its tree annual LAI values indicate which vegetation  
116 type dominates. To classify the vegetation type in a Tropical Evergreen Forest, the dominant PFT should  
117 be a tropical broadleaf evergreen tree with annual mean leaf area index in upper canopy ( $LAI_{upper}$ ) above  
118  $2.5 \text{ m}^2 \text{ m}^{-2}$ . To classify the vegetation type in a Tropical Deciduous Forest, the dominant PFT should be  
119 a tropical broadleaf drought-deciduous tree with annual mean  $LAI_{upper}$  above  $2.5 \text{ m}^2 \text{ m}^{-2}$ . For ecosystems  
120 where no tree PFT is dominant, the tree LAI between  $0.8$  and  $2.5 \text{ m}^2 \text{ m}^{-2}$  characterizes savannas, and  
121 values smaller than  $0.8 \text{ m}^2 \text{ m}^{-2}$  characterize a grassland vegetation type.

122 We assume that the vegetation types Tropical Evergreen Forest and the Tropical Deciduous Forest  
123 in INLAND represent the Amazon rainforest, while Savanna and Grasslands represent the Cerrado.  
124 Savanna would be equivalent to the Cerrado physiognomies *Cerradão* and *Cerrado sensu strictu*, while  
125 Grasslands would be equivalent to the physiognomies *Campo sujo* and *Campo Limpo* (*sensu* Ribeiro and  
126 Walter, 2008).

127 The soil chemical properties are represented by the carbon cycle (C), nitrogen (N) and phosphorus  
128 (P). The carbon cycle is simulated through vegetation, litter and soil organic matter, where the  
129 biogeochemical module is similar to the CENTURY model (Parton et al., 1993; Verberne et al., 1990).  
130 The amount of C existing in the first meter of soil is divided into different compartments characterized  
131 by their residence time, which can vary in an interval of hours for microbial biomass and organic matter  
132 to several years for lignin. For the nitrogen, the model considers only the soil N transformations and  
133 carbon decomposition, not influencing the productivity of vegetation, i.e., there is a fixed C:N ratio.



134 Phosphorus is used only to limit the gross primary productivity. The total phosphorus available in the soil  
135 ( $P_{total}$ ) is used to estimate the maximum capacity of carboxylation by the Rubisco enzyme ( $V_{max}$ ) through  
136 a linear relationship (Castanho et al., 2013).

$$137 \quad V_{max} = 0.1013 P_{total} + 30.037 \quad (1)$$

138 where  $V_{max}$  and  $P_{total}$  are given in  $\mu\text{molCO}_2 \text{ m}^{-2} \text{ s}^{-1}$  and  $\text{mg kg}^{-1}$ , respectively.

139 INLAND also contains two fire model options for simulation. The first is a simple fixed-value  
140 disturbance, which does not depend on the environmental conditions. The second is dynamic and based  
141 on the fire module of the Canadian model of fire CTEM (Arora and Boer, 2005). In this module, all three  
142 aspects of the fire triangle – the availability of fuel to burn, the flammability of vegetation depending on  
143 environmental conditions, and the presence of an ignition source – are considered. It uses an arbitrary  
144 anthropogenic fire probability which is added to the natural ignition probability. Only the dynamical fire  
145 module is used in this study.

## 146 **2.3 Observed data**

### 147 **2.3.1 Phosphorus databases**

148 We used two phosphorus databases to estimate  $V_{max}$  (Equation 1): one regional and one global  
149 database (referred to as PR and PG, respectively). In addition, a control phosphorus map (PC) represents  
150 the unlimited nutrient availability case, equivalent to a  $V_{max}$  of  $65 \mu\text{molCO}_2 \text{ m}^{-2} \text{ s}^{-1}$ , or  $350 \text{ mg P kg}^{-1}$  soil,  
151 according to Equation 1.

152 The regional phosphorus database (PR) was developed from total phosphorus in the soil for the  
153 Amazon basin published by Quesada et al. (2011) plus 54 additional available phosphorus samples (P





154 extracted via Mehlich-1 extractor) (Figure 2a). We used the  $P_{\text{mehlich-1}}$  and clay contents measured in a  
155 forest-savanna transition region in Brazil (Mato Grosso state) to estimate  $P_{\text{total}}$  and expand the coverage  
156 area of the phosphorus data (Section S1). These 54 samples were gridded to a  $1^\circ \times 1^\circ$  grid to be compatible  
157 with the spatial resolution used by INLAND, resulting in 12 new pixels with information of the total  
158 phosphorus content (Figure 2a). For pixels without  $P_{\text{total}}$  information, the PR dataset considered  $P_{\text{total}}$  equal  
159 to  $350 \text{ mg P kg}^{-1}$  soil, similarly to the PC conditions.

160 A global dataset of total phosphorus content in the soil ( $P_{\text{total}}$ ) was also used (Figure 2b). This  
161 global total phosphorus data is part of a database containing six global maps of the different forms of  
162 phosphorus in the soil (Yang et al., 2013). The total phosphorus was estimated from lithologic maps,  
163 distribution of soil development stages, fraction of the remaining source material for different stages of  
164 weathering using chronosequence studies (29 studies), and phosphorus distribution in different forms for  
165 each soil type based on the analysis of Hedley fractionation (Yang and Post, 2011), which are part of a  
166 worldwide collection of soil profile data. According to Yang et al. (2013), the uncertainties and limitations  
167 of this database are restricted to the Hedley fractionation data used. When quantified, these uncertainties  
168 are 17% for low weathered soils, 65% for intermediate soils and 68% for highly weathered soils.

### 169 2.3.2 Above-Ground Biomass (AGB) database

170 The AGB database used was created by Nogueira et al. (2015) and considers a vegetation  
171 originally existing in the Brazilian Amazonia. This database was based on a vegetation map at a scale of  
172 1:250000 (IBGE, 1992) and biomass averages from 41 published studies that had conducted direct  
173 sampling in either forest (2317 plots) or non-forest or contact zones (1830 plots). We bilinearly



174 interpolated the AGB (dry weight) for each transect considering  $1^\circ \times 1^\circ$  to ensure compatibility of the  
175 observed and simulated data.

176 The five-fixed longitudinal transects (Figure 1) were used separately to characterize vegetation  
177 from AGB in the Amazon-Cerrado border (Figures 3a and 3b). These transects were also compared to the  
178 simulated results considering the different combinations among all treatments.

179 In general, the higher AGB values in the west and lower values in the east for T1, T2, T3 and T4  
180 are consistent with the transition from a dense and woody vegetation towards a sparse vegetation with  
181 lower biomass, typical of the Amazon-Cerrado border (Figure 3a). However, in T1, a gradual reduction  
182 of biomass along the west to east gradient is shown, differently than T2, T3 and T4 where the biomass  
183 decreases abruptly. In T5 no west-east gradient is present with high biomass heterogeneity and  
184 predominant low biomass across the transect (Figure 3b).

185 In the north of the Amazon-Cerrado border (T1), the duration of the dry season is smaller and the  
186 annual rainfall is higher in comparison to other transects. This region is characterized by the presence of  
187 transitional forest formations, such as dense forest and a transitional deciduous/semideciduous forest.  
188 These forest formations are common in the south of Tocantins state, where water is not limiting, the soils  
189 are sandy and the surface is flat (Haidar et al., 2013). Thus, the less pronounced biomass decline could  
190 feature the transition from two forest formations with different structures. On the other hand, T5 located  
191 at the south of the transition border, is exposed to longer dry season duration and stronger precipitation  
192 seasonality. Despite its lower biomass, T5 presents a high AGB spatial variability (Figure 3b). Due to its  
193 greater territorial extent (880 km) in the Cerrado domain, different types of vegetation have been sampled,  
194 featuring a mixed medium-sized and small vegetation. Moreover, different soil and topographical settings



195 are found, featuring a highly heterogeneous landscape in this region (Silva et al., 2006). For example, in  
196 the Cerrado domain, the vegetation structure varies substantially within and between vegetation types,  
197 and generally has been associated with soil spatial patterns, landform and drainage (Silva et al. 2006).

## 198 **2.4 Simulations**

199 The model was forced with prescribed climate based on the Climate Research Unit (CRU)  
200 database (Harris et al., 2014). Two climate boundary conditions were used: the first is referred to as the  
201 monthly climatological average (CA) that represents the average climate of 1961-1990. The second  
202 climate boundary condition is the historical dataset, for the continuous period between 1948 and 2008  
203 (CV). For both boundary conditions, the variables used are rainfall, solar radiation, wind velocity and  
204 maximum and minimum temperatures. The dataset has a 1-degree spatial resolution and a monthly time  
205 resolution.

206 Soil texture data is based on the IGBP-DIS global soil (Global Soil Data Task 2000) (Hansen and  
207 Reed, 2000). The model simulations were run for a total period of 427 years. An initial spin up of 366  
208 years was used to initialize the carbon pools to equilibrium (equivalent to the period 1582-1947), when  
209 the climate data for 1948-2008 was applied cyclically, plus the period of 1948-2008.

210 The experiment design was based on the combination of climate scenarios (CA, climatological  
211 average, 1961-1990; CV, monthly climate data, 1948-2008), variable atmospheric CO<sub>2</sub> concentration  
212 (from 278 to 380 ppm), the nutrient limitation on V<sub>max</sub> (PC, no phosphorus limitation  
213 (V<sub>max</sub> = 65 μmolCO<sub>2</sub> m<sup>-2</sup> s<sup>-1</sup>); PR, regional phosphorus limitation; PG, global phosphorus limitation) and  
214 the occurrence of fire effects (F) or not (Table 1).



215           These combinations allow the evaluation of individual and combined effects of climate, soil  
216 chemistry, and the incidence of fire in the total productivity of the ecosystems, tree biomass and LAI, and  
217 their effects on the location of the Amazon-Cerrado border.

218           We simulated the individual effects of climate variability, phosphorus limitation and fire on the  
219 variables: Net Primary Production (NPP), tree biomass, and LAI of the upper and lower canopies  
220 ( $LAI_{upper}$ ,  $LAI_{lower}$ ).

221           The analysis of the isolated effects of climate variability was performed using a combination of  
222 CV+PC and CA+PC. We consider that the subtraction between the simulations  $(CV+PC)-(CA+PC) =$   
223  $(CV-CA)|_{PC}$  represents the effect of climate variability if phosphorus limitations are not considered.

224           The same logic was applied to isolate other factors such as fire and phosphorus in different climate  
225 scenarios. For example, the isolated effect of fire with an average climate scenario without the influence  
226 of phosphorus limitation is calculated by the difference between  $CA+PC+F$  and  $CA+PC$ , so that  
227  $(CA+PC+F) - (CA+PC) = F|_{CA, PC}$ . The isolated effect of fire with a climate variability scenario without  
228 influence of P limitation is calculated by the difference between  $CV+PC+F$  and  $CV+PC$ , so that  
229  $(CV+PC+F) - (CV+PC) = F|_{CV, PC}$ . The different combinations of climate scenarios with or without the  
230 fire effect and different phosphorus limitations are described in Table 2.

## 231 **2.5 Statistical analysis and determination of the best model configuration**

232           The variables tested are NPP, LAI and AGB. The statistical analysis is divided in four parts. First,  
233 we present maps with the spatial patterns of isolated effects for all simulated area, and the differences  
234 between the treatments that are statistically significant at  $p < 0.05$  (according to the t-test) are shaded.



235           Second, we present an analysis of variance using the one-way ANOVA and the Tukey-Kramer  
236 test in the transition zone. To this end, we grouped treatments according to climate (Group 1), nutrient  
237 limitation (Group 2) and presence or absence of fire (Group 3). In Group 1 we tested if CA and CV results  
238 were significantly different from each other along the transects, regardless of nutrient limitation,  
239 presence or absence of fire. Similarly, in Group 2 we organize the simulations according to the type of  
240 nutrient limitation, PC, PR or PG, regardless of climate, and presence or absence of fire. In Group 3 the  
241 simulations were grouped considering fire presence or no fire. Finally, all treatments were tested  
242 individually to assess the effects on NPP, LAI and AGB.

243           Third, a correlation coefficient between the simulated and observed values for AGB was  
244 calculated for each transect. The simulated variables are averaged for the last 10 years of simulations  
245 (1999 - 2008) and compared to biomass from Nogueira et al. (2015) within a grid cell.

246           Finally, we evaluate INLAND's ability to assign the type of dominant vegetation analyzing 10  
247 years of probability of occurrence. If the dominant vegetation type (evergreen tropical forest or deciduous  
248 forest for the Amazon rainforest, and savanna or grasslands for Cerrado) in a pixel is the same in more  
249 than 90% of the simulated years (9 of 10), then the simulated vegetation type is defined as "very robust"  
250 for that pixel; if it occurs in 70 - 90% of the simulated years, it is considered to be "robust". If the dominant  
251 vegetation occurred in less than 70% of simulated years, the pixel is considered "transitional" vegetation.



## 252 3 Results

### 253 3.1 Influence of climate, fire and phosphorus in the Amazon-Cerrado transition region

#### 254 3.1.1 Spatial patterns

255 Overall, the inclusion of climate interannual variability (CV) resulted in a decrease in the  
256 simulated average biomass by 3.8% in Amazonia, and by 8.7% in Cerrado in comparison to average  
257 climate (CA) (Figure 4a). The differences between CV and CA AGB simulations are statistically  
258 significant and range from  $-3 \text{ kg-C m}^{-2}$  to  $2 \text{ kg-C m}^{-2}$ . The state of Pará, where geographically there is  
259 higher influence of El Niño phenomenon, presented the highest decrease in AGB in CV simulation. In  
260 the state of Roraima, on the other hand, there was an increase of about  $2 \text{ kg-C m}^{-2}$  in AGB when CV was  
261 considered. Bolivia and southwest of Mato Grosso state also presented, in some grids points, a significant  
262 increase in AGB higher than  $2 \text{ kg-C m}^{-2}$ .

263 The phosphorus total concentration acts in average as a limiting factor in the tree biomass. Biomass  
264 decreased by 13% in regional phosphorus database (PR) and 15% in global phosphorus database (PG). In  
265 PR, biomass decreased mainly in the southeastern Amazonia (between Pará and northeastern of Mato  
266 Grosso states) and northwestern Amazonas state (Figure 4b). In PG, the largest declines in biomass  
267 occurred in central Amazonia, northeastern Pará and northeastern Mato Grosso (Figure 4c). In Cerrado,  
268 on the other hand, tree biomass declined by 2% and 9% in relation to control simulation when PR and PG  
269 were considered, respectively. In PR the few pixels in the Cerrado that have nutrient limitation showed a  
270 significant decrease in tree biomass (Figure 4b), but in PG on the other hand, our results showed biomass  
271 reduction statistically significant for most of the Cerrado domain, except only for the southern Tocantins



272 state (Figure 4c), reinforcing the hypothesis that phosphorus limitation influences the vegetation structure  
273 and landscape, and that we need to implement P cycles in tropical ecosystems modeling.

274 Fire effect declines tree biomass with largest magnitude and intensity than phosphorus limitation  
275 or interannual climate variability (Figure 4d), as expected. The small or null fire effect in the Central  
276 Amazon rainforest shows that the Amazonia forest is naturally inflammable as well as a gradient towards  
277 seasonally dryer climate that increases the intensity and magnitude of fire effects towards the Cerrado  
278 (Figure 4d). The fire effect over the Amazon domain was 8-9% of the P limitation effect (PR and PG,  
279 respectively), while the fire effect over the Cerrado was over 250% of the P effects. This magnitude  
280 characterizing the quickly increase of grasses after fire occurrence in the latter.

### 281 **3.1.2 Influence of climate, fire and phosphorus in the transects**

282 Results of the ANOVAs and Tukey–Kramer test indicate that the inclusion of climate interannual  
283 variability (CV), limitation by phosphorus (PR and PG) and fire in INLAND model led to significantly  
284 different averages of NPP, LAI and biomass in transition zone. This influence of climate, phosphorus and  
285 fire are shown separately in Tables 3 to Table 5 and combined in Table 6.

286 The effects of climate and phosphorus on productivity show that CV reduce the NPP from 0.68  
287  $\text{kg-C m}^{-2} \text{yr}^{-1}$  to 0.64  $\text{kg-C m}^{-2} \text{yr}^{-1}$  (Table 3) and the phosphorus effect (PR and PG) result in biomass  
288 decline from 0.71  $\text{kg-C m}^{-2} \text{yr}^{-1}$  and 0.64  $\text{kg-C m}^{-2} \text{yr}^{-1}$ , respectively (Table 4). The fire effect, moreover,  
289 has a positive effect increasing the NPP from 0.66  $\text{kg-C m}^{-2} \text{yr}^{-1}$  and 0.67  $\text{kg-C m}^{-2} \text{yr}^{-1}$  for PR and PG,  
290 that although it is low, is statistically significant according to Tukey Kramer test (Table 5).

291 The same relationship was found in  $\text{LAI}_{\text{total}}$  and  $\text{LAI}_{\text{upper}}$  where CV and nutrient limitation reduce  
292 the  $\text{LAI}_{\text{total}}$  in the canopy (Table 3 and Table 4). For  $\text{LAI}_{\text{total}}$  the effect of fire is positive, increasing tree



293 times  $LAI_{lower}$  and increasing  $LAI_{upper}$  (Table 5). In biomass, the magnitude of fire effect is greater in  
294 relation to the climate variability and nutritional limitation effects. While climate variability introduced  
295 changes in the order of 5% for AGB (Table 3) and phosphorus changes of up to 14% (Table 4), fire  
296 decreased AGB by 46.7% (Table 5).

297 The results of NPP and AGB for CV+PC simulation, do not present significant difference from  
298 CA+PC (Table 6) which does not agree with Table 3.  $LAI_{total}$  and  $LAI_{upper}$  have significant reduction for  
299 transitional area when interannual climate variability was considered, which could be improve the  
300 INLAND vegetation classification results.

301 The inclusion of P limitation in INLAND simulations (CV+PR and CV+PG) without fire  
302 occurrence caused significant decline in relation CV+PC for all variables (NPP, AGB, and  $LAI_{total}$ ), but  
303 no difference between them (PR, PG) (Table 6).

304 Fire effects are significant only for structural variables as AGB,  $LAI_{total}$ ,  $LAI_{upper}$  and  $LAI_{lower}$ . It  
305 presents an increase of  $LAI_{total}$  of  $1.52 \text{ m}^2 \text{ m}^{-2}$  in CV+PG+F in relation to CV+PG, and of  $1.32 \text{ m}^2 \text{ m}^{-2}$  in  
306 CV+PR+F in relation to CV+PR (Table 6). This increment of LAI corresponds to the increase of grasses  
307 and the decrease of trees.

### 308 3.1.3 West-East patterns of AGB in the Amazon-Cerrado transition

309 The model used in this study simulates > 80% of the observed biomass variability in all treatments  
310 along the transition area except in T5 (Table 7). It shows that the model is able to capture biomass  
311 variability along the transition area, which is relevant when compared to recent studies that validate the  
312 representation of models in the Amazon using biomass observation data (Senna et al., 2009; Castanho et  
313 al., 2013).





314 It is not possible to identify a treatment that best represents the biomass of all transects (Table 7).  
315 A combined analysis of Table 7 and Figure 5 indicates a general agreement that biomass decreases from  
316 W to E in T1 to T4, and this is well captured by several configurations of the model, with specific  
317 differences among them. Overall, CA and PC configurations yield higher biomass, while the introduction  
318 of interannual climate variability (CV), phosphorus limitations (PG) and fire (F) reduces the biomass.  
319 However, the simulated results may be above or below the observed ones, which suggests an additional  
320 local factor not included in the model.

321 Most likely, errors may have occurred in the representation of soil physical properties, which are  
322 very important in the calculation of moisture stress.

323 The curves of AGB (Figure 5) shows the impact of CV, phosphorus limitation and fire along the  
324 West-East transition. The AGB gradient of CA+PC and CV+PC are similar in all transects showing that  
325 in the transition the climate interannual variability into the model has little influence on vegetation  
326 structure. On the other hand, the phosphorus limitation presented high influence in the transition,  
327 decreasing the AGB especially in the grids in the west transects, where the Amazon vegetation is  
328 predominant. This influence could be easily observed in T3 and T4, where PG decrease the AGB by  
329  $2 \text{ kg-C m}^{-2}$  in the west of the transects (Figure 5). In T1, T2 and T5 AGB decline is also higher when P  
330 was incorporated in relation the curves limited only by CV. For these transects INLAND represents the  
331 gradient of dense vegetation structure towards a sparse vegetation decreasing the AGB along the transects.  
332 In T1, model simulations tend to underestimate the highest and the lowest biomass extremes, despite of  
333 the improvement in the correlation with the inclusion of the fire component the absolute values were all  
334 underestimated in this transect.



335 Fire, however in T2, T3 and T4, is responsible to approach the simulated biomass to the observed  
336 biomass in the east grids into Cerrado domain. In T5, these relations are similar, with climate presenting  
337 less influence on biomass decrease than phosphorus, and fire appears mainly as a reducer factor.

### 338 **3.2 Simulated composition of vegetation**

339 Most of the pixels in CA show very robust simulations, with more than 90% of the same vegetation  
340 cover in the last 10 years simulated (Figure 6a-c and 6g-i). A larger number of pixels with values below  
341 70% of agreement of vegetation type were simulated when considering CV. An even higher variability in  
342 CV compared to CA simulations was observed when we added the effects of phosphorus limitation and  
343 fire.

344 The vegetation composition in all nutrient limitation scenarios for CA simulations resulted in  
345 >90% of agreement on the vegetation type for nearly all pixels, except for the north of Cerrado domain  
346 (Figures 6a, 6b and 6c). CA+PC and CA+PR simulations had the same vegetation composition, while  
347 CA+PG replaced the deciduous forest by evergreen forest in the central Cerrado region, around 8° S 46°  
348 W (Figures 6A, 6B and 6C). Cerrado was better represented in CV+PC, CV+PR and CV+PG than in the  
349 same CA combinations (Figure 6). The occurrence of forested areas in the central Cerrado decreased in  
350 CV combinations, these being replaced by the savanna or grassland vegetation class.

351 When the effect of fire was added to CA simulations, the model simulated an increase in the  
352 uncertainty on the vegetation cover classification in the Cerrado region. The effect of fire reduced the  
353 presence of deciduous forest in central Cerrado biome as well as in CA+PC, and the vegetation was  
354 replaced by evergreen forest and savanna in CA+PC+F (Figures 6G, 6H, 6I). In CV simulations, fire



355 effect results in the replacement of the deciduous and perennial forest by savanna and grasses in all central  
356 Cerrado region (Figures 6J, 6K and 6L).

357 Transitional forest areas in the northern Tocantins state (TO) and southeastern Mato Grosso (MT)  
358 are not adequately represented. With >90% of concordance, INLAND assigns the existence of tropical  
359 evergreen forest rather than deciduous forest in TO for all combinations used, and the existence of tropical  
360 evergreen forest rather than savanna in MT, indicating difficulty in simulating transitional vegetation in  
361 this place.

#### 362 **4 Discussion**

363 The inclusion of climate interannual variability (CV), limitation by phosphorus (PR and PG) and  
364 fire in INLAND model led to significantly different averages of tree biomass (Figure 4) and aboveground  
365 biomass (Table 6), which agrees with the consensus that these factors influence vegetation structure in  
366 the forest-savanna border (Hoffmann et al., 2012; Dantas et al., 2013; Lehmann et al., 2014; Baudena et  
367 al., 2015). In this work, the spatial analysis and the Tukey-Kramer test (TK) results show that there is a  
368 difference in magnitude among these factors in vegetation, with fire occurrence and phosphorus limitation  
369 being stronger than climate interannual variability (Figure 4).

370 CV declines biomass predominantly in eastern Amazonia (Figure 4a). In this region, the El Niño–  
371 Southern Oscillation (ENSO) phenomenon could reduce by 50% the amount of rainfall, putting the  
372 vegetation under intense water stress (Botta and Foley, 2002). This change in interannual rainfall brings  
373 in direct changes in carbon flux and stocks in leaves and wood leading changes in vegetation structure.

374 The differences between CA and CV were significant for most part of these biomes, except central  
375 Amazonia (Figure 4a), where the climate interannual variability and seasonality of precipitation have



376 been pointed as secondary effect on vegetation, since there is no shortage of water availability during the  
377 dry season (Restrepo-Coupe et al., 2013). However, although CV has a significant effect on AGB in our  
378 region-wide results (Figure 4a), there is no significant difference along the transects in the Amazon-  
379 Cerrado transition (Table 6). This difference occurred because a smaller sample size was used to test CV  
380 in each simulation. In Table 6, the difference between CA+PC and CV+PC is around  $0.30 \text{ kg-C m}^{-2}$ , not  
381 significant at  $\alpha=0.05$ . On the other hand, when we analyzed the influence of CV in the same place, but  
382 using all simulations, regardless of phosphorus limitation and fire occurrence, the results showed a  
383 significant decrease in AGB by  $0.38 \text{ kg-C m}^{-2}$  in the transition (Table 3). Thus, we conclude that CV has  
384 influence on the vegetation structure, but its magnitude is so small along the transition that it is not  
385 detected by Tukey-Kramer test in the CV+PC simulation. Thus, compared to P limitation and fire  
386 occurrence, CV has a secondary role. It was expected, since a seasonal climate region, such as the  
387 Amazon-Cerrado transition, suffers less influence of interannual oscillations in precipitation and the  
388 vegetation is likely more adapted to the water stress.

389 Along the Cerrado, lower water availability in CV affects tree biomass although that vegetation is  
390 predominantly grassy-herbaceous. The biomass decline is significant for most part of the simulated  
391 Cerrado domain (Figure 4a) and average values could reduce by half the amount of tree biomass in  
392 Amazonia. In this biome, the shallow soils, high porosity and the fine root biomass exposed the few trees  
393 to higher water stress compared to the Amazon in dry years (Ruggeiro et al., 2002).

394 Phosphorus limitation effect was statistically significant for PR and PG along all the Amazon  
395 domain and the main differences between these simulations were the spatial patterns of tree biomass  
396 decrease (Figure 4b and Figure 4c). We cannot affirm which of these databases are better because they



397 are the results of different methodologies and observations (Yang et al., 2014; Quesada et al., 2009).  
398 However, we observe that PG showed a higher biomass decrease in central Amazonia, northeastern Pará  
399 and northeastern Mato Grosso, indicating that in these areas the phosphorus limitation is higher. This  
400 result does not corroborate the northwest-southeast AGB gradient found in the Amazon basin, which is a  
401 result of higher productivity in the west where soils are more fertile than those found in the southeast  
402 (Aragão et al., 2009; Saatchi et al., 2007; Nunes et al., 2012; Lee et al., 2013). On the other hand, PR  
403 biomass agrees with the northwest-southeast gradient, presenting less limitation in the soils of central  
404 Amazonia with declines in biomass mainly in the southeastern Amazonia (between Pará and northeastern  
405 of Mato Grosso states) (Figure 4b).

406 In Cerrado, phosphorus limitation also limited vegetation when was considered in model  
407 simulations (Figure 4c) and presented statistically significant differences in relation to CV+PC. In this  
408 biome, as well as in the Amazon, tree abundance has been generally associated with increases of soil  
409 fertility (Vourtilis et al., 2013). Richness and diversity of vegetation was correlated with soil fertility  
410 (Long et al., 2012), and highlight the importance of P in the composition and maintenance of vegetation,  
411 especially in transition areas.

412 Compared to the Amazon domain, the effects of phosphorus limitation is lower in the Cerrado,  
413 probably due to the adaptation of savanna species to the P-restrictions caused by a lack of an effective  
414 and robust nutrient cycling system compared to the forests (Oliveira et al. *in press*). In PR, the few pixels  
415 that have nutrient limitation showed a significant decrease in arboreal biomass (Figure 4b), but in PG, our  
416 results showed reduction of biomass statistically significant for most of the Cerrado domain, except only  
417 for the southern Tocantins state (Figure 4c). Despite the differences in spatial patterns, there was no



418 statistically significant differences between PR and PG within the transects (Table 4) showing that there  
419 is little difference in west-east gradient of soil fertility and that INLAND has small sensitivity to the  
420 different P databases used.

421 The spatial difference between the global phosphorus database (PG) and the regional phosphorus  
422 database (PR) showed that PG underestimates total phosphorus in the western Amazonia, and  
423 overestimates in northern Amazonia with respect to PR. Moreover, PG presented underestimates in south  
424 of the transition and overestimates in Cerrado domain and northeast of transition at transects limits when  
425 compared to PR (Figure S1). These differences show that the understanding of phosphorus influence  
426 limitation, on vegetation is directly associated to reliability of databases and reveal the need to improve  
427 the data set for  $P_{\text{total}}$  in the soils of the Amazon and Cerrado/Amazon transition domains.

428 The  $P_{\text{total}}$  versus  $V_{\text{max}}$  linear relationship is a proxy of the influence of soil fertility in  
429 photosynthesis, not considering the phosphorus-soil-vegetation feedback. To our knowledge, none of the  
430 current Dynamic Global Vegetation Models DGVMs considers the complete cycle of phosphorus, despite  
431 the importance of nutrient cycling for the biomass maintenance and dynamics of the tropical vegetation  
432 in dystrophic soils. For example, nutrient cycling in the Amazon/Cerrado transition is close related to the  
433 hyperdynamic turnover of the biomass (Valadão et al. 2016), in which some key species might also be  
434 key to the hypercycling of nutrients through which vegetation sustain the constant input of nutrients,  
435 including large annual amounts of available P (Oliveira et al. *in press*).

436 The decrease in tree biomass occasioned by phosphorus limitation can contribute to a decrease  
437 in litter production and consequently could affect the nutrient cycling in tropical ecosystems. According  
438 to Oliveira et al. (*in press*), the litter produced by vegetation corresponds to the main return route to the



439 available fraction of phosphorus for plants, especially in the transition areas, where  $P_{\text{available}}$  in the soil is  
440 very low. In our model, however, phosphorus acts directly in the photosynthesis limitation through  $V_{\text{max}}$   
441 and cannot be reabsorbed by the roots. Thus, the litter produced in vegetation contribute only to dry matter  
442 and fire occurrence increase. The litter affected by fire occurrence volatilizes the small amount of  
443 phosphorus available to plants, increasing the nutrient losses of the ecosystem. Despite this simplified  
444 representation in INLAND, it is clear that phosphorus has a significant effect on woody biomass in the  
445 Amazon and Cerrado and that biomass spatial variability is fully associated with the P variability in the  
446 soil (Figure 4b and Figure 4c).

447 The comparison between (CV+PG)–(CV+PG+F) showed that Amazon vegetation remains  
448 naturally impervious to fire (Figure 4d), contrary to the tropical savannas, which are naturally affected by  
449 this disturbance, followed by natural recover (i.e. resilience) (Lehmann et al., 2011; Murphy and  
450 Bowman, 2012; Lehmann et al., 2014). The fire occurrence along the Amazon-Cerrado border is  
451 influenced by the gradient from a dense forest towards a seasonal and/or semi deciduous forest, or a sparse  
452 vegetation type like savanna.

453 Our results confirm our hypothesis showing fire as an important factor controlling the biomass  
454 dynamic (Silvério et al., 2013; Couto-Santos et al., 2014; Balch et al., 2015), with statistically significant  
455 influences (Table 5). The fire effect may reduce AGB by 50% in the transition zone, which under climate  
456 change or deforestation conditions, may lead to an even stronger change in the vegetation structure and  
457 dynamic.

458 In the Cerrado domain, the fire effect implies in significant increases of shrubs and herbaceous  
459 vegetation and decreases of the arboreal component. The Cerrado, however, is relatively resilient to fire



460 depending on the velocity, intensity and duration of the burning (Rezende et al., 2005; Elias et al., 2013  
461 Reis et al., 2015). The adaptive morphological nature and the low nutrient requirement of vegetation allow  
462 Cerrado the ability to rapidly restore the vegetation after fire occurrence (Hoffmann et al., 2005;  
463 Hoffmann et al., 2012).

464 In the transect zone, our model was able to represent the variability of the biomass. Compared to  
465 previous modeling studies, our study shows an improvement in the correlations between simulated and  
466 observed AGB. Senna et al. 2009 found 0.20 as maximum correlation coefficient between simulated and  
467 observed ABG while Castanho et al. (2013) showed 0.80 for Amazonia domain. In this study, the  
468 correlation coefficients for ABG are usually above 0.80 for the transects, regardless of the treatment,  
469 except for T5 (Table 7).

470 It is clear that interannual climate variability, fire occurrence and phosphorus limitation in the  
471 transition zone reduce the biomass and play significant roles in the simulations (Figure 5), but the only  
472 inclusion of these effects is still insufficient to represent the actual vegetation structure in the Amazon-  
473 Cerrado border. In our interpretation, this means that other important factors are still missing from the  
474 simulation, and that our P dataset and fire module need to be improved. A better spatial representation of  
475 soil physical properties, including shallow rocky soils, as well as physiological characteristics of the  
476 vegetation as carbon allocation, deciduousness of vegetation, and residence time are probably needed to  
477 improve this simulation.

478 In the transects, the influence of climate interannual variability (CV+PC), P limitation (CV+PG)  
479 and fire (CV+PG+F) on AGB are also evident, when compared to the control simulation (CA+PC) and  
480 to the observed data (Figure 5). For all transects the biomass curves have similar patterns, where the





481 smaller difference is observed between CA+PC and CV+PG curves, while the larger difference is when  
482 fire is incorporated in the Amazon. The effect of phosphorus limitation appears as an intermediate effect  
483 reducing the biomass more than the effect of climate variability. In Cerrado, it is observed that there is  
484 little or no difference among biomass simulated by CA+PC, CV+PC and CV+PG, revealing that in this  
485 biome, interannual climate variability and phosphorus have smaller influence in the vegetation structure.  
486 However, in the east of T2, T3 and T4, fire is the factor that adjusts the simulated to the observed data  
487 (Figure 5), differently than the grid points in the west, where CV+PG is a better proxy between observed  
488 and simulated data.

489 Such conditions are interesting because reflects the different mechanisms that regulates these  
490 ecosystems and probably the phytophysiognomies distribution. For example, P limitation seems to be the  
491 factor that improves biomass simulated in regions where the predominant vegetation type is the tropical  
492 rainforest. Fire, on the other hand, improves the biomass in grid points where the Cerrado occurs.  
493 Moreover, important factors such as productivity partitioning into leaves, roots and wood carbon pools  
494 are assumed to be fixed in space and time within a given PFT, neglecting the natural capacity of  
495 transitional forests to adapt itself and to adjust their metabolism to seasonal climate conditions (Senna et  
496 al., 2009). In years of severe drought, transitional forests could prioritize the stock of carbon to fine roots  
497 instead of the basal increment in order to maximize access to available water, or make hydraulic  
498 redistribution to maintain the greenness and photosynthesis rates (Figure 5a). Brando et al. (2008) found  
499 high sensitivity in carbon allocation for eastern Amazon basin trees, which reduced wood production by  
500 13-60% in response to an artificial drought. Although in INLAND soil moisture is able to reduce the



501 photosynthetic rates during the months of lower rainfall, it does not dynamically change the allocation  
502 rates, exposing the PFTs to severe water stress and underestimating the biomass (Figure 5a).

503 Along this seasonal climate, located in the central region of the Amazon-Cerrado transition, T3  
504 and T4 showed the highest average correlations between observed and simulated data (Table 7). For these  
505 transects, INLAND is able to capture the high variability of biomass gradient. However, the AGB in the  
506 Cerrado grid points of these transects are underestimated due to the lower water availability in this  
507 environment (Figure 5b and Figure5d).

508 At the T5 transect located at the south of the transition, the average correlations were low for all  
509 treatments, indicating that INLAND has difficulty to represent the AGB gradient there (Table 7).  
510 However, it captures the lower biomass as compared to the northern ones. In this region, the vegetation  
511 is characterized by a wide diversity of physiognomies, which varies with other preponderant factors, such  
512 as lithology, soil depth, topography and fertility. The observed data also showed high biomass variability,  
513 indicating that there are changes in the vegetation structure, featuring medium-sized and small vegetation  
514 types on different soil types. In INLAND, however, features such as lithology and water-table depth are  
515 not considered due to the complexity of its representation on the large scale, limiting the representation  
516 of a heterogeneous environment throughout the transition. Thus, we observe for T5 transect an  
517 underestimated biomass and a high variability along the west-east gradient.

518 Overall, we observe that different patterns of vegetation distribution along the Amazon-Cerrado  
519 border exist and are influenced not only by climate variability, phosphorus limitation, and fire, but also  
520 by ecophysiological parameters, which have different behavior according to the environmental conditions  
521 and soil proprieties. Obtaining these parameters is a challenge to the scientific community once the field



522 measurements are difficult due to the extension of the transition area. More observed data are needed to  
523 establish and implement the plasticity of the fixed parameters such as carbon coefficients allocation,  
524 residence time, dependence of the deciduousness to phosphorus, and others, to improve the representation  
525 of the Amazon-Cerrado limits, since the model showed that it is able to represent the average behavior of  
526 the transition.

527         The simulation of the spatial distribution of vegetation types by INLAND also improved when  
528 climate, phosphorus limitation and fire were considered. The simulations with CV showed a decrease in  
529 evergreen forests areas into Cerrado domain with replacement by tropical deciduous forest and Savanna  
530 (Figure 6). The inclusion of fire in CV simulations brings an improvement along the Amazon-Cerrado  
531 border, enlarging the savanna vegetation type and decreasing forests areas into Cerrado border domain.  
532 The best combination found to represent the frontier of the Amazon-Cerrado was CV+PG+F (climate  
533 variability + global map of phosphorus limitation + fire occurrence). Although CV+PC+F and CV+PR+F  
534 presented similar vegetation types to CV+PG+F, the latter showed more robust results in the Cerrado  
535 domain. On the other hand, in the absence of fire, the main factor driving the distribution of vegetation in  
536 terms of biomass and consequently of phytophysiognomic types, becomes the availability of P in the soil.  
537 Therefore, the fire dynamic is the preponderant factor controlling the dynamics and shifts of the  
538 vegetation in the Amazon/Cerrado transition zone

## 539 **5 Conclusions**

540         This is the first study that assesses the modelling representation of the Amazon-Cerrado border.  
541 This study shows that, although INLAND forced by a climatological database is able to simulate basic  
542 characteristics of the Amazon-Cerrado transition and that adding factors such as climate interannual



543 variability, phosphorus limitation and fire gradually improves simulated vegetation types, improvements  
544 are still needed. These effects are not homogeneous along the latitudinal/longitudinal gradient, which  
545 makes the adequate simulation of biomass challenging in some places along the transition. Our work  
546 shows that there is a synergistic effect between these variables in Amazonia-Cerrado transition and that,  
547 in terms of magnitude, the effect of fire is stronger than the nutrient restriction and climate, resulting in  
548 the main determinant factor of the vegetation changes along the transition. The nutrient limitation in turn  
549 is stronger than the effect of climate variability acting on the dynamics of transitional ecosystems,  
550 therefore determining the vegetation distribution in the absence of fire.

551 Overall, although INLAND typically simulates more than 80% of the variability of biomass in the  
552 transition zone, in many places the biomass is clearly not well simulated. Situations for wet or dry  
553 conditions were well simulated, but the simulations are generally poor for transitional areas where the  
554 environment selected physiognomies that have an intermediate behavior, as is the case of the transitional  
555 forests in northern Tocantins and Mato Grosso. The lack of field parameters measured in the transition  
556 zone is still a major limitation to improve the DGVMs. Spatially explicit carbon allocation strategies,  
557 mortality rates, physiological and structural parameters are necessary to establish numerical relationships  
558 between the environment and the vegetation dynamic models to make them able to correctly simulate  
559 current patterns and future changes in vegetation considering future climate change. In addition, it is also  
560 needed to include not only the spatial variability, but also temporal variability in physiological parameters  
561 of vegetation, allowing a more realistic simulation of the vegetation-climate relationship. Finally, our  
562 results reinforce the importance and need of the DGVMs to incorporate the nutrient limitation and fire  
563 occurrence to obtain more realistic results.



564 **6 Acknowledgements**

565 We gratefully thank FAPEMIG and CAPES for their financial support.

566 **7 References**

567 Aragão, L. E. O. C., Malhi, Y., Metcalfe, D. B., Silva-Espejo, J. E., Jiménez, E., Navarrete, D.,  
568 Almeida, S., Costa, A. C. L., Salinas, N., Phillips, O. L., Anderson, L. O., Baker, T. R., Goncalvez, P. H.,  
569 Huamán-Ovalle, J., Mamani-Solórzano, M., Meir, P., Monteagudo, A., Peñuela, M. C., Prieto, A.,  
570 Quesada, C. A., Rozas-Dávila, A., Rudas, A., Silva Junior, J. A. and Vásquez, R.: Above- and below-  
571 ground net primary productivity across ten Amazonian forests on contrasting soils, *Biogeosciences*, 6,  
572 2441–2488, doi:10.5194/bgd-6-2441-2009, 2009.

573 Arora, V. K. and Boer, G. J.: A parameterization of leaf phenology for the terrestrial ecosystem  
574 component of climate models, *Glob. Chang. Biol.*, 11, 39–59, doi:10.1111/j.1365-2486.2004.00890.x,  
575 2005.

576 Balch, J. K., Brando, P. M., Nepstad, D. C., Coe, M. T., Silvério, D., Massad, T. J., Davidson, E.  
577 A., Lefebvre, P., Oliveira-Santos, C., Rocha, W., Cury, R. T. S., Parsons, A. and Carvalho, K. S.: The  
578 Susceptibility of Southeastern Amazon Forests to Fire: Insights from a Large-Scale Burn Experiment,  
579 *Bioscience*, 65(9), 893–905, doi:10.1093/biosci/biv106, 2015.

580 Baudena, M., Dekker, S. C., Van Bodegom, P. M., Cuesta, B., Higgins, S. I., Lehsten, V., Reick,  
581 C. H., Rietkerk, M., Scheiter, S., Yin, Z., Zavala, M. A. and Brovkin, V.: Forests, savannas, and  
582 grasslands: Bridging the knowledge gap between ecology and Dynamic Global Vegetation Models,  
583 *Biogeosciences*, 12(6), 1833–1848, doi:10.5194/bg-12-1833-2015, 2015.



584 Betts, R. A., Cox, P. M., Collins, M., Harris, P. P., Huntingford, C. and Jones, C. D.: The role of  
585 ecosystem-atmosphere interactions in simulated Amazonian precipitation decrease and forest dieback  
586 under global climate warming, *Theor. Appl. Climatol.*, 78, 157–175, doi:10.1007/s00704-004-0050-y,  
587 2004.

588 Bonan, G. B.: Forests and climate change: forcings, feedbacks, and the climate benefits of forests,  
589 *Science*, 320(5882), 1444–1449, doi:10.1126/science.1155121, 2008.

590 Botta, A. and Foley, J. A.: Effects of climate variability and disturbances on the Amazonian  
591 terrestrial ecosystems dynamics, *Global Biogeochem. Cycles*, 16(4), doi:10.1029/2000GB001338, 2002.

592 Brando, P. M., Nepstad, D. C., Davidson, E. A., Trumbore, S. E., Ray, D. and Camargo, P.:  
593 Drought effects on litterfall, wood production and belowground carbon cycling in an Amazon forest:  
594 results of a throughfall reduction experiment, *Philos. Trans. R. Soc. Lond. B. Biol. Sci.*, 363(1498), 1839–  
595 48, doi:10.1098/rstb.2007.0031, 2008.

596 Castanho, A. D. A., Coe, M. T., Costa, M. H., Malhi, Y., Galbraith, D. and Quesada, C. A.:  
597 Improving simulated Amazon forest biomass and productivity by including spatial variation in  
598 biophysical parameters, *Biogeosciences*, 10(4), 2255–2272, doi:10.5194/bg-10-2255-2013, 2013.

599 Couto-Santos, F. R., Luizão, F. J. and Carneiro Filho, A.: The influence of the conservation status  
600 and changes in the rainfall regime on forest-savanna mosaic dynamics in Northern Brazilian Amazonia,  
601 *Acta Amaz.*, 44(2), 197–206, 2014.

602 Cox, P. M., Betts, R. A., Jones, C. D., Spall, S. A. and Totterdell, I. J.: Acceleration of global  
603 warming due to carbon-cycle feedbacks in a coupled climate model, *Nature*, 408(November), 184–187,  
604 doi:10.1038/35041539, 2000.



605 Cox, P. M., Betts, R. A., Collins, M., Harris, P. P., Huntingford, C. and Jones, C. D.: Amazonian  
606 forest dieback under climate-carbon cycle projections for the 21st century, *Theor. Appl. Climatol.*, 78,  
607 137–156, doi:10.1007/s00704-004-0049-4, 2004.

608 Dajoz, R.: *Princípios de ecologia*, 7<sup>o</sup> edição, Artmed, Porto Alegre, RS, Brazil 519pp, 2005.

609 Dantas, V. L., Batalha, M. A. and Pausas, J. G.: Fire drives functional thresholds on the savanna-  
610 forest transition, *Ecology*, 94(11), 2454–2463, doi:10.1890/12-1629.1, 2013.

611 Elias, F., Marimon, B. S., Matias, S. R. A., Forsthofer, M., Morandi, P. S. and Marimon-junior,  
612 B. H.: Dinâmica da distribuição espacial de populações arbóreas, ao longo de uma década, em cerrado  
613 na transição Cerrado-Amazônia, *Mato Grosso, Biota Amaz.*, 3, 1–14, 2013.

614 Favier, C., Chave, J., Fabing, A., Schwartz, D. and Dubois, M. A.: Modelling forest-savanna  
615 mosaic dynamics in man-influenced environments: Effects of fire, climate and soil heterogeneity, *Ecol.*  
616 *Modell.*, 171, 85–102, doi:10.1016/j.ecolmodel.2003.07.003, 2004.

617 Foley, J. A., Prentice, I. C., Ramankutty, N., Levis, S., Pollard, D., Sitch, S. and Haxeltine, A.: An  
618 integrated biosphere model of land surface processes, terrestrial carbon balance, and vegetation dynamics,  
619 *Global Biogeochem. Cycles*, 10, 603, doi:10.1029/96GB02692, 1996.

620 Goedert, W: *Solos do Cerrado: Tecnologias e Estratégias de Manejo*, Empresa Brasileira de  
621 *Pesquisa Agropecuária (EMBRAPA)*, Brasília, DF, Brasil. 422pp., 1986.

622 Haidar, R. F., Fagg, J. M. F., Pinto, J. R. R., Dias, R. R., Damasco, G., Silva, L. D. C. R. and Fagg,  
623 C. W.: Florestas estacionais e áreas de ecótono no estado do Tocantins, Brasil : parâmetros estruturais ,  
624 classificação das fitofisionomias florestais e subsídios para conservação, *Acta Amaz.*, 43(3), 261–290,  
625 doi:10.1590/S0044-59672013000300003, 2013.



- 626 Hansen, M. C. and Reed, B.: A comparison of the IGBP DISCover and University of Maryland  
627 1km global land cover products, *Int. J. Remote Sens.*, 21, 1365–1373, doi:10.1080/014311600210218,  
628 2000.
- 629 Harris, I., Jones, P. D., Osborn, T. J. and Lister, D. H.: Updated high-resolution grids of monthly  
630 climatic observations - the CRU TS3.10 Dataset, *Int. J. Climatol.*, 34(3), 623–642, doi:10.1002/joc.3711,  
631 2014.
- 632 Hirota, M., Nobre, C., Oyama, M. D. and Bustamante, M. M. C.: The climatic sensitivity of the  
633 forest, savanna and forest-savanna transition in tropical South America, *New Phytol.*, 187, 707–719,  
634 doi:10.1111/j.1469-8137.2010.03352.x, 2010.
- 635 Hoffmann, W. A., Da Silva, E. R., Machado, G. C., Bucci, S. J., Scholz, F. G., Goldstein, G. and  
636 Meinzer, F. C.: Seasonal leaf dynamics across a tree density gradient in a Brazilian savanna, *Oecologia*,  
637 145, 307–316, doi:10.1007/s00442-005-0129-x, 2005.
- 638 Hoffmann, W. A., Geiger, E. L., Gotsch, S. G., Rossatto, D. R., Silva, L. C. R., Lau, O. L.,  
639 Haridasan, M. and Franco, A. C.: Ecological thresholds at the savanna-forest boundary: How plant traits,  
640 resources and fire govern the distribution of tropical biomes, *Ecol. Lett.*, 15, 759–768,  
641 doi:10.1111/j.1461-0248.2012.01789.x, 2012.
- 642 House, J. I., Archer, S., Breshears, D. D. and Scholes, R. J.: Conundrums in mixed woody-  
643 herbaceous plant systems, *J. Biogeogr.*, 30, 1763–1777, doi:10.1046/j.1365-2699.2003.00873.x, 2003.
- 644 IBGE.: *Manual Técnico da Vegetação Brasileira (Manuais Técnicos em Geociências n. 1)*,  
645 Fundação Instituto Brasileiro de Geografia e Estatística (IBGE), Rio de Janeiro, RJ, Brasil. 92pp., 1992.





- 646 IBGE.: Mapa da Vegetação do Brasil, Fundação Instituto Brasileiro de Geografia e Estatística  
647 (IBGE), Rio de Janeiro, RJ, Brazil, Map, 2004.
- 648 Klink, C. A. and Machado, R. B.: Conservation of the Brazilian Cerrado, *Conserv. Biol.*, 19(3),  
649 707–713, doi:10.1111/j.1523-1739.2005.00702.x, 2005.
- 650 Kucharik, C. J., Foley, J. A., Delire, C., Fisher, V. A., Coe, M. T., Lenters, J. D., Young-Molling,  
651 C., Ramankutty, N., Norman, J. M. and Gower, S. T.: Testing the performance of a Dynamic Global  
652 Ecosystem Model: Water balance, carbon balance, and vegetation structure, *Global Biogeochem. Cycles*,  
653 14(3), 795–825, doi:10.1029/1999GB001138, 2000.
- 654 Lee, J. E., Frankenberg, C., van der Tol, C., Berry, J. A., Guanter, L., Boyce, C. K., Fisher, J. B.,  
655 Morrow, E., Worden, J. R., Asefi, S., Badgley, G. and Saatchi, S.: Forest productivity and water stress in  
656 Amazonia: observations from GOSAT chlorophyll fluorescence, *Proc. R. Soc. B Biol. Sci.*, 280(1761),  
657 20130171–20130171, doi:10.1098/rspb.2013.0171, 2013.
- 658 Lehmann, C. E. R., Archibald, S. A., Hoffmann, W. A. and Bond, W. J.: Deciphering the  
659 distribution of the savanna biome, *New Phytol.*, 191, 197–209, doi:10.1111/j.1469-8137.2011.03689.x,  
660 2011.
- 661 Lehmann, C. E. R., Anderson, T. M., Sankaran, M., Higgins, S. I., Archibald, S., Hoffmann, W.  
662 A., Hanan, N. P., Williams, R. J., Fensham, R. J., Felfili, J., Hutley, L. B., Ratnam, J., Jose, J. S., Montes,  
663 R., Franklin, D., Russell-Smith, J., Ryan, C. M., Durigan, G., Hiernaux, P., Haidar, R., Bowman, D. M.  
664 J. S., Bond, W. J., San Jose, J., Montes, R., Franklin, D., Russell-Smith, J., Ryan, C. M., Durigan, G.,  
665 Hiernaux, P., Haidar, R., Bowman, D. M. J. S. and Bond, W. J.: Savanna Vegetation-Fire-Climate



666 Relationships Differ Among Continents, *Science*, 343 (January), 548–553, doi:10.1126/science.1247355,  
667 2014.

668 Long, W., Yang, X. and Donghai, L.: Patterns of species diversity and soil nutrients along a  
669 chronosequence of vegetation recovery in Hainan Island, South China, *Ecol. Res.*, 2012.

670 Malhi, Y., Aragão, L. E. O. C., Metcalfe, D. B., Paiva, R., Quesada, C. A., Almeida, S., Anderson,  
671 L., Brando, P., Chambers, J. Q., da Costa, A. C. L., Hutyyra, L. R., Oliveira, P., Patiño, S., Pyle, E. H.,  
672 Robertson, A. L. and Teixeira, L. M.: Comprehensive assessment of carbon productivity, allocation and  
673 storage in three Amazonian forests, *Glob. Chang. Biol.*, 15, 1255–1274, doi:10.1111/j.1365-  
674 2486.2008.01780.x, 2009.

675 Marimon Junior, B. H. and Haridasan, M.: Comparação da vegetação arbórea e características  
676 edáficas de um cerradão e um cerrado sensu stricto em áreas adjacentes sobre solo distrófico no leste de  
677 Mato Grosso, Brasil, *Acta Bot. Brasilica*, 19(4), 913–926, doi:10.1590/S0102-33062005000400026,  
678 2005.

679 Marimon, B. S., Lima, E. S., Duarte, T. G., Chieregatto, L. C., Ratter, J. A.: Observations on the  
680 vegetation of northeastern Mato Grosso, Brazil. IV. An analysis of the Cerrado-Amazonian Forest  
681 ecotone, *Edinburgh Journal of Botany*, 63, 323–341, doi: 10.1017/S0960428606000576, 2006.

682 Marimon, B. S., Marimon-Junior, B. H., Feldpausch, T. R., Oliveira-Santos, C., Mews, H. A.,  
683 Lopez-Gonzalez, G., Lloyd, J., Franczak, D. D., de Oliveira, E. A., Maracahipes, L., Miguel, A., Lenza,  
684 E. and Phillips, O. L.: Disequilibrium and hyperdynamic tree turnover at the forest–cerrado transition  
685 zone in southern Amazonia, *Plant Ecol. Divers.*, 7(1–2), 281–292, doi:10.1080/17550874.2013.818072,  
686 2014.



687 Mercado, L. M., Patino, S., Domingues, T. F., Fyllas, N. M., Weedon, G. P., Sitch, S., Quesada,  
688 C. A., Phillips, O. L., Aragao, L. E. O. C., Malhi, Y., Dolman, A. J., Restrepo-Coupe, N., Saleska, S. R.,  
689 Baker, T. R., Almeida, S., Higuchi, N. and Lloyd, J.: Variations in Amazon forest productivity correlated  
690 with foliar nutrients and modelled rates of photosynthetic carbon supply, *Philos. Trans. R. Soc. Lond. B.*  
691 *Biol. Sci.*, 366(1582), 3316–3329, doi:10.1098/rstb.2011.0045, 2011.

692 Morandi, P.S., Marimon-Junior, B. H., Oliveira, E. A., Reis, S. M. A., Valadão, M. B. X.,  
693 Forsthofer, M., Passos, F. B., Marimon, B. S.: Vegetation Succession in the Cerrado-Amazonian Forest  
694 Transition Zone of Mato Gross State, Brazil, *Edinburgh Journal of Botany*, 73, 83-93, doi:  
695 10.1017/S096042861500027X, 2016.

696 Moreno, M. I. C., Schiavini, I. and Haridasan, M.: Fatores edáficos influenciando na estrutura de  
697 fitofisionomias do cerrado, *Caminhos da Geogr.*, 9(25), 173–194, 2008.

698 Murphy, B. P. and Bowman, D. M. J. S.: What controls the distribution of tropical forest and  
699 savanna?, *Ecol. Lett.*, 15, 748–758, doi:10.1111/j.1461-0248.2012.01771.x, 2012.

700 Myers, N., Fonseca, G. A. B., Mittermeier, R. A., Fonseca, G. A. B. and Kent, J.: Biodiversity  
701 hotspots for conservation priorities, *Nature*, 403(6772), 853–858, doi:10.1038/35002501, 2000.

702 Nardoto, G. B., Bustamante, M. M. C., Pinto, A. S. and Klink, C. A. Nutrient use efficiency at  
703 ecosystem and species level in savanna areas of Central Brazil and impacts of fire, *J. Trop. Ecol.*, 22,  
704 191–201, doi:10.1017/S0266467405002865, 2006.

705 Nogueira, E. M., Yanai, A. M., Fonseca, F. O. and Fearnside, P. M.: Carbon stock loss from  
706 deforestation through 2013 in Brazilian Amazonia, *Glob. Chang. Biol.*, doi:10.1111/gcb.12798, 2015.



707 Nunes, E. L., Costa, M. H., Malhado, A. C. M., Dias, L. C. P., Vieira, S. A., Pinto, L. B. and Ladle,  
708 R. J.: Monitoring carbon assimilation in South America's tropical forests: Model specification and  
709 application to the Amazonian droughts of 2005 and 2010, *Remote Sens. Environ.*, 117, 449–463,  
710 doi:10.1016/j.rse.2011.10.022, 2012.

711 Oliveira, B., Marimon-Junior, B. H., Mews, H. A., Valadão, M. B. X., Marimon, B. S.:  
712 Unravelling the ecosystem functions in the Amazonia-Cerrado transition: evidence of hyperdynamic  
713 nutrient cycling, *Plant Ecol.*, *in press*, doi: 10.1007/s11258-016-0681-y

714 Oyama, M. D. and Nobre, C. A.: A new climate-vegetation equilibrium state for Tropical South  
715 America, *Geophys. Res. Lett.*, 30(23), 10–13, doi:10.1029/2003GL018600, 2003.

716 Parton, W. J., Scurlock, J. M. O., Ojima, D. S., Gilmanov, T. G., Scholes, R. J., Schimel, D. S.,  
717 Kirchner, T., Menaut, J.-C., Seastedt, T., Garcia Moya, E., Kamnalrut, A. and Kinyamario, J. I.:  
718 Observations and modeling of biomass and soil organic matter dynamics for the grassland biome  
719 worldwide, *Global Biogeochem. Cycles*, 7, 785, doi:10.1029/93GB02042, 1993.

720 Pereira, M. P. S., Malhado, A. C. M. and Costa, M. H.: Predicting land cover changes in the  
721 Amazon rainforest: An ocean-atmosphere-biosphere problem, *Geophys. Res. Lett.*, 39(9),  
722 doi:10.1029/2012GL051556, 2012.

723 Pires, G. F. and Costa, M. H.: Deforestation causes different subregional effects on the Amazon  
724 bioclimatic equilibrium, *Geophys. Res. Lett.*, 40(14), 3618–3623, doi:10.1002/grl.50570, 2013.

725 Quesada, C. A., Lloyd, J., Schwarz, M., Baker, T. R., Phillips, O. L., Patiño, S., Czimczik, C.,  
726 Hodnett, M. G., Herrera, R., Arneeth, A., Lloyd, G., Malhi, Y., Dezzeo, N., Luizão, F. J., Santos, A. J. B.,  
727 Schmerler, J., Arroyo, L., Silveira, M., Priante Filho, N., Jimenez, E. M., Paiva, R., Vieira, I., Neill, D.



728 A., Silva, N., Peñuela, M. C., Monteagudo, A., Vásquez, R., Prieto, A., Rudas, A., Almeida, S., Higuchi,  
729 N., Lezama, A. T., López-González, G., Peacock, J., Fyllas, N. M., Alvarez Dávila, E., Erwin, T., di Fiore,  
730 A., Chao, K. J., Honorio, E., Killeen, T., Peña Cruz, A., Pitman, N., Núñez Vargas, P., Salomão, R.,  
731 Terborgh, J. and Ramírez, H.: Regional and large-scale patterns in Amazon forest structure and function  
732 are mediated by variations in soil physical and chemical properties, *Biogeosciences Discuss.*, 6, 3993–  
733 4057, doi:10.5194/bgd-6-3993-2009, 2009.

734 Quesada, C. A., Lloyd, J., Anderson, L. O., Fyllas, N. M., Schwarz, M. and Czimczik, C. I.: Soils  
735 of Amazonia with particular reference to the RAINFOR sites, *Biogeosciences*, 8, 1415–1440,  
736 doi:10.5194/bg-8-1415-2011, 2011.

737 Quesada, C. A., Phillips, O. L., Schwarz, M., Czimczik, C. I., Baker, T. R., Patiño, S., Fyllas, N.  
738 M., Hodnett, M. G., Herrera, R., Almeida, S., Alvarez Dávila, E., Arneeth, A., Arroyo, L., Chao, K. J.,  
739 Dezzeo, N., Erwin, T., Di Fiore, A., Higuchi, N., Honorio Coronado, E., Jimenez, E. M., Killeen, T.,  
740 Lezama, A. T., Lloyd, G., López-González, G., Luizão, F. J., Malhi, Y., Monteagudo, A., Neill, D. A.,  
741 Núñez Vargas, P., Paiva, R., Peacock, J., Peñuela, M. C., Peña Cruz, A., Pitman, N., Priante Filho, N.,  
742 Prieto, A., Ramírez, H., Rudas, A., Salomão, R., Santos, A. J. B., Schmerler, J., Silva, N., Silveira, M.,  
743 Vásquez, R., Vieira, I., Terborgh, J. and Lloyd, J.: Basin-wide variations in Amazon forest structure and  
744 function are mediated by both soils and climate, *Biogeosciences*, 9(6), 2203–2246, doi:10.5194/bg-9-  
745 2203-2012, 2012.

746 Reis, S. M., Marimon, B. S., Marimon Junior, B.-H., Gomes, L., Morandi, P. S., Freire, E. G. and  
747 Lenza, E.: Resilience of savanna forest after clear-cutting in the Cerrado-Amazon transition zone,  
748 *Bioscience*, 31(5), 1519–1529, doi:10.14393/BJ-v31n5a2015-26368, 2015.



749 Restrepo-Coupe, N., da Rocha, H. R., Hutyrá, L. R., da Araujo, A. C., Borma, L. S.,  
750 Christoffersen, B., Cabral, O. M. R., de Camargo, P. B., Cardoso, F. L., da Costa, A. C. L., Fitzjarrald,  
751 D. R., Goulden, M. L., Kruijt, B., Maia, J. M. F., Malhi, Y. S., Manzi, A. O., Miller, S. D., Nobre, A. D.,  
752 von Randow, C., S, L. D. A., Sakai, R. K., Tota, J., Wofsy, S. C., Zanchi, F. B. and Saleska, S. R.: What  
753 drives the seasonality of photosynthesis across the Amazon basin? A cross-site analysis of eddy flux tower  
754 measurements from the Brazil flux network, *Agric. For. Meteorol.*, 182–183, 128–144,  
755 doi:10.1016/j.agrformet.2013.04.031, 2013.

756 Rezende, A. V., Sanquetta, C. R. and Filho, F. A.: Efeito do desmatamento no estabelecimento de  
757 espécies lenhosas em um cerrado *Sensu stricto*, *Floresta*, 35, 69–88, 2005.

758 Ribeiro, J. F. and Walter, B. M. T.: As Principais Fitofisionomias do bioma Cerrado, in *Cerrado:*  
759 *ecologia e flora*, pp. 153–212., 2008.

760 Rocha, H. R. da, Goulden, M. L., Miller, S. D., Menton, M. C., Pinto, L. D. V. O., De Freitas, H.  
761 C. and Figueira, A. M. E. S.: Seasonality of water and heat fluxes over a tropical forest in eastern  
762 Amazonia, *Ecol. Appl.*, 14(4 SUPPL.), doi:10.1890/02-6001, 2004.

763 Roy, S. B. and Avissar, R.: Impact of land use/land cover change on regional hydrometeorology  
764 in Amazonia, *J. Geophys. Res.*, 107(D20), 1–12, doi:10.1029/2000JD000266, 2002.

765 Ruggiero, P. G. C., Batalha, M. A., Pivello, V. R. and Meirelles, S. T.: Soil-vegetation  
766 relationships in cerrado (Brazilian savanna) and semideciduous forest, Southeastern Brazil, *Plant Ecol.*,  
767 160(1), 1–16, doi:10.1023/A:1015819219386, 2002.



768 Saatchi, S., Houghton, R. A., Dos Santos Alvalá, R. C., Soares, J. V. and Yu, Y.: Distribution of  
769 aboveground live biomass in the Amazon basin, *Glob. Chang. Biol.*, 13(4), 816–837, doi:10.1111/j.1365-  
770 2486.2007.01323.x, 2007.

771 Salazar, L. F., Nobre, C. A. and Oyama, M. D.: Climate change consequences on the biome  
772 distribution in tropical South America, *Geophys. Res. Lett.*, 34(April), 2–7, doi:10.1029/2007GL029695,  
773 2007.

774 Senna, M. C. A., Costa, M. H., Pinto, L. I.C., Imbuzeiro, H. M. A., Diniz, L. M. F. and Pires, G.  
775 F.: Challenges to reproduce vegetation structure and dynamics in Amazonia using a coupled climate-  
776 biosphere model, *Earth Interact.*, 13(11), doi:10.1175/2009EI281.1, 2009.

777 Shukla, J., Nobre, C. and Sellers, P.: Amazon deforestation and climate change, *Science*, 247,  
778 1322–1325, doi:10.1126/science.247.4948.1322, 1990.

779 Silva, J. F., Fariñas, M. R., Felfili, J. M. and Klink, C. A.: Spatial heterogeneity, land use and  
780 conservation in the cerrado region of Brazil, in *Journal of Biogeography*, vol. 33, pp. 536–548., 2006.

781 Silvério, D. V., Brando, P. M., Balch, J. K., Putz, F. E., Nepstad, D. C., Oliveira-Santos, C. and  
782 Bustamante, M. M. C.: Testing the Amazon savannization hypothesis: fire effects on invasion of a  
783 neotropical forest by native cerrado and exotic pasture grasses, *Philos. Trans. R. Soc. Lond. B. Biol. Sci.*,  
784 368, 20120427, doi:10.1098/rstb.2012.0427, 2013.

785 Torello-Raventos, M., Feldpausch, T., Veenendaal, E., Schrodte, F., Saiz, G., Domingues, T.,  
786 Djagbletey, G., Ford, A., Kemp, J., Marimon, B., Hur Marimon Junior, B., Lenza, E., Ratter, J.,  
787 Maracahipes, L., Sasaki, D., Sonké, B., Zapfack, L., Taedoumg, H., Villarroel, D., Schwarz, M., Quesada,  
788 C., Yoko Ishida, F., Nardoto, G., Affum-Baffoe, K., Arroyo, L., Bowman, D., Compaore, H., Davies, K.,



789 Diallo, A., Fyllas, N., Gilpin, M., Hien, F., Johnson, M., Killeen, T., Metcalfe, D., Miranda, H., Steininger,  
790 M., Thomson, J., Sykora, K., Mougín, E., Hiernaux, P., Bird, M., Grace, J., Lewis, S., Phillips, O. and  
791 Lloyd, J.: On the delineation of tropical vegetation types with an emphasis on forest/savanna transitions,  
792 *Plant Ecol. Divers.*, 6, 101–137, doi:10.1080/17550874.2012.76281, 2013.

793 Valadão, M. B. X., Marimon-Junior, B. H., Oliveira, B., Lúcio, N. W., Souza, M. G. R., Marimon,  
794 B. S.: Biomass hyperdynamic as a key modulator of forest self-maintenance in dystrophic soil at  
795 Amazonia-Cerrado transition. *Scientia Forestalis*, 44, 475-485, 2016.

796 Veenendaal, E. M., Torello-Raventos, M., Feldpausch, T. R., Domingues, T. F., Gerard, F.,  
797 Schrodte, F., Saiz, G., Quesada, C. A., Djangbletey, G., Ford, A., Kemp, J., Marimon, B. S., Marimon-  
798 Junior, B. H., Lenza, E., Ratter, J. A., Maracahipes, L., Sasaki, D., Sonk, B., Zapfack, L., Villarroel, D.,  
799 Schwarz, M., Yoko Ishida, F., Gilpin, M., Nardoto, G. B., Affum-Baffoe, K., Arroyo, L., Bloomfield, K.,  
800 Ceca, G., Compaore, H., Davies, K., Diallo, A., Fyllas, N. M., Gignoux, J., Hien, F., Johnson, M., Mougín,  
801 E., Hiernaux, P., Killeen, T., Metcalfe, D., Miranda, H. S., Steininger, M., Sykora, K., Bird, M. I., Grace,  
802 J., Lewis, S., Phillips, O. L. and Lloyd, J.: Structural, physiognomic and above-ground biomass variation  
803 in savanna-forest transition zones on three continents - How different are co-occurring savanna and forest  
804 formations?, *Biogeosciences*, 12(10), 2927–2951, doi:10.5194/bg-12-2927-2015, 2015.

805 Verberne, E. L. J., Hassink, J., De Willigen, P., Groot, J. J. R. and Van Veen, J. A.: Modelling  
806 organic matter dynamics in different soils, *Netherlands J. Agric. Sci.*, 38, 221–238, 1990.

807 Vourlitis, G. L., de Lobo, F. A., Lawrence, S., de Lucena, I. C., Pinto, O. B., Dalmagro, H. J.,  
808 Ortiz, C. E. and de Nogueira, J. S.: Variations in Stand Structure and Diversity along a Soil Fertility





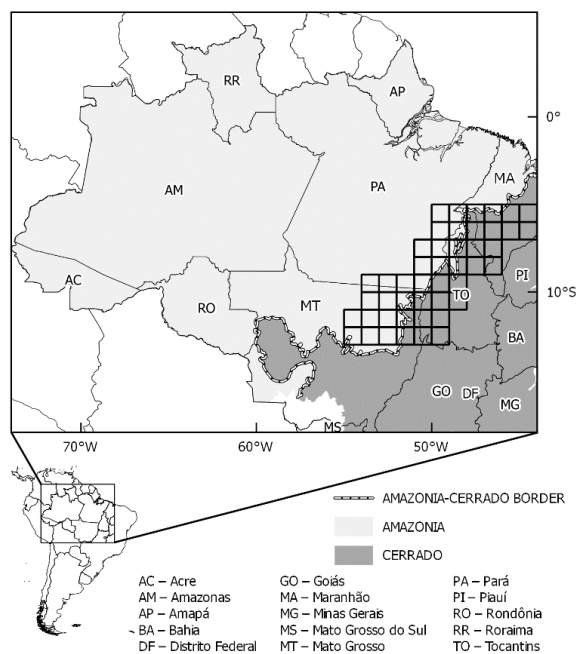
809 Gradient in a Brazilian Savanna (Cerrado) in Southern Mato Grosso, *Soil Sci. Soc. Am. J.*, 77(4), 1370–  
810 1379, doi:10.2136/sssaj2012.0336, 2013.

811 Yang, X. and Post, W. M.: Phosphorus transformations as a function of pedogenesis: A synthesis  
812 of soil phosphorus data using Hedley fractionation method, *Biogeosciences*, 8, 2907–2916,  
813 doi:10.5194/bg-8-2907-2011, 2011.

814 Yang, X., Post, W. M., Thornton, P. E. and Jain, A.: The distribution of soil phosphorus for global  
815 biogeochemical modeling, *Biogeosciences*, 10, 2525–2537, doi:10.5194/bg-10-2525-2013, 2013.

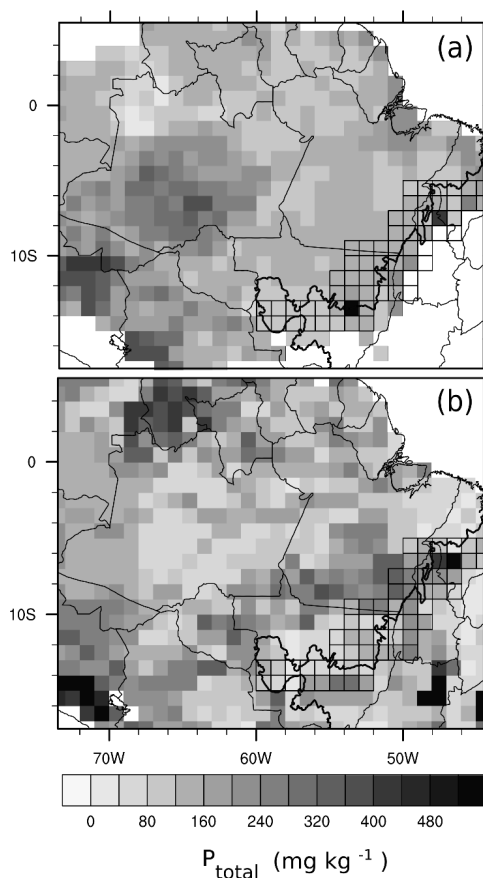
816 Yang, X., Thornton, P. E., Ricciuto, D. M. and Post, W. M.: The role of phosphorus dynamics in  
817 tropical forests - A modeling study using CLM-CNP, *Biogeosciences*, 11, 1667–1681, doi:10.5194/bg-  
818 11-1667-2014, 2014.

819



820

821 **Figure 1.** Delimitation of the study area Amazonia (in light gray) and Cerrado (in dark gray) (IBGE  
822 (2004), and the location of five transects used in this work (from T1 to T5). The dashed line represents  
823 the border between biomes.

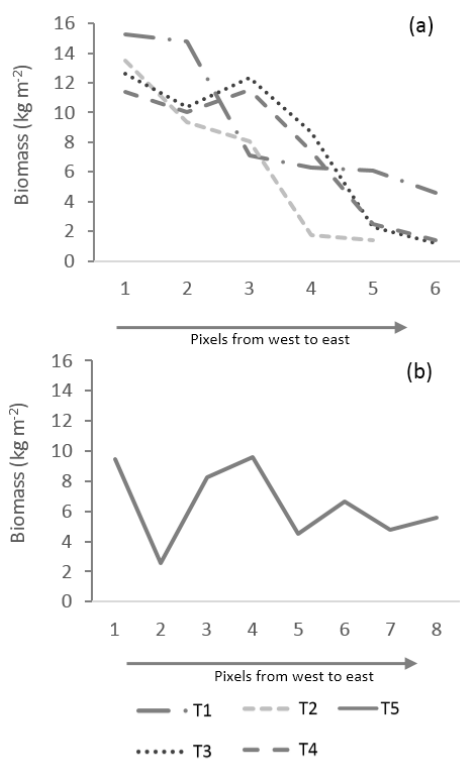


824

825 **Figure 2.** (a) Map of regional total phosphorus in the soil with new estimated  $P_{\text{total}}$  data - PR, (b)

826 Map of global total phosphorus in the soil (Yang et al., 2013) – (PG).

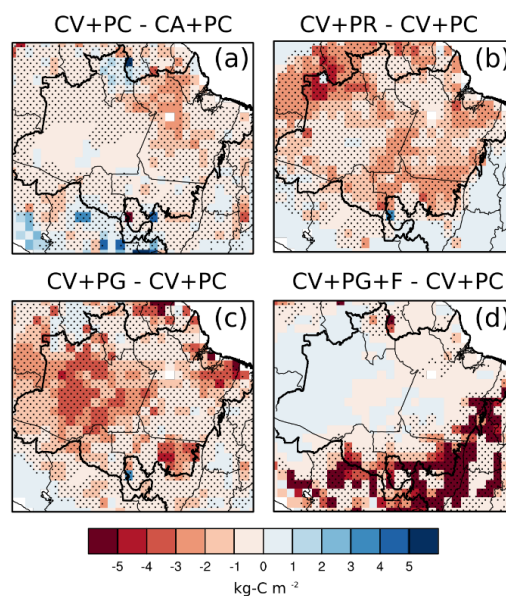
827



828

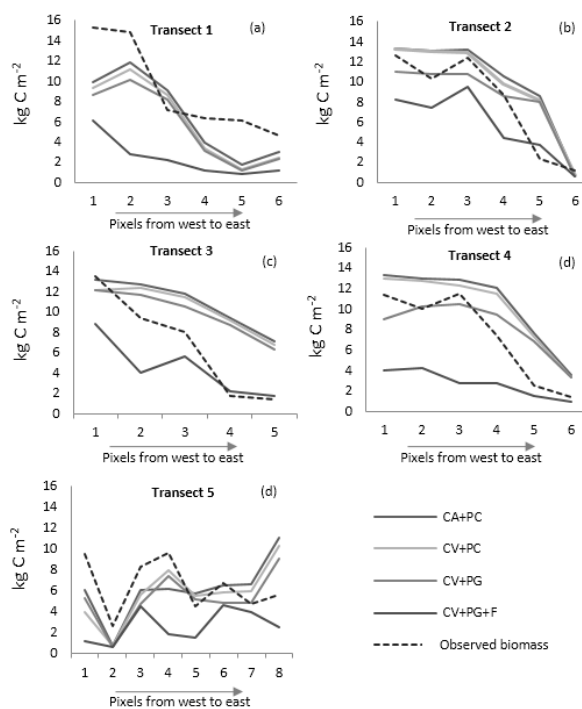
829 **Figure 3.** West-East patterns of AGB in the Amazonia-Cerrado transition for the five transects

830 analyzed.



831

832 **Figure 4.** Interannual climate variability effect (a), Regional phosphorus limitation effect (b), Global  
 833 phosphorus limitation effect (c), and fire effect (d) on tree biomass. The hatched areas indicate that the  
 834 variables are significantly different compared to the control simulation at the level of 95% according to  
 835 the t-test and the thick black line is the geographical limits of the biomes.

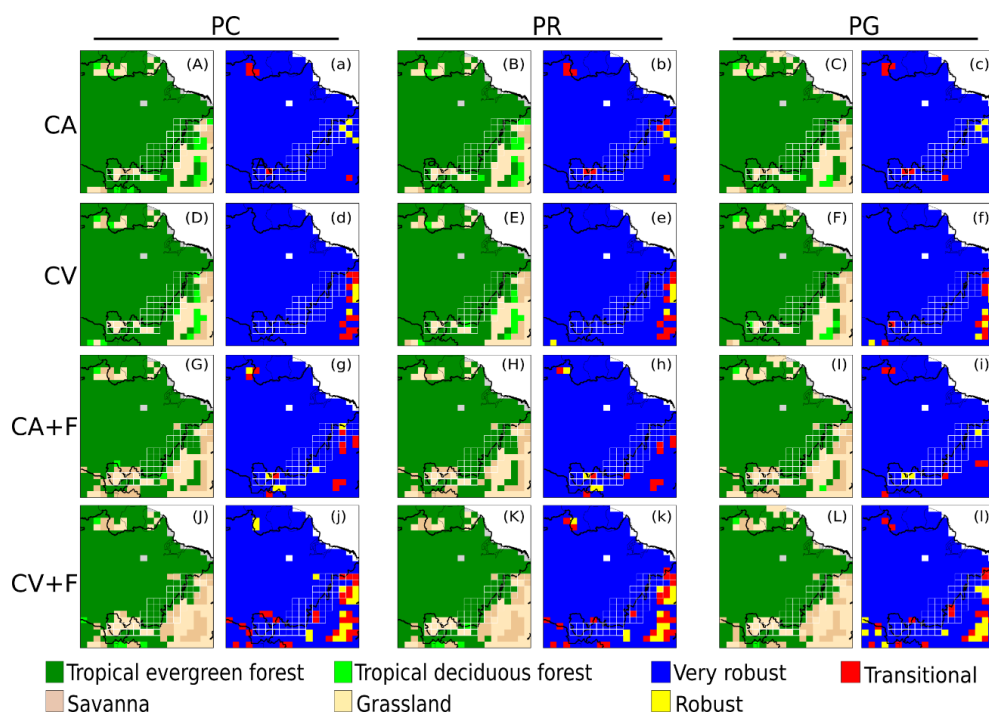


836

837 **Figure 5.** Longitudinal biomass gradient in Amazonia-Cerrado transition simulated for T1 to T5  
838 considering different combinations: observed data; seasonal climate control simulation (CA+PC);  
839 interannual climate variability (CV+PC); interannual climate variability + global phosphorus limitation  
840 (CV+PG); and interannual climate variability + phosphorus + fire occurrence (CV+PG+F).



841



842

843 **Figure 6.** Results for the dominant vegetation cover simulated by INLAND for the different treatments  
 844 (A-L) and a metric of variability of results (a-l). Simulations are considered very robust if the dominant  
 845 vegetation agrees on 9-10 of the last 10 years of simulation, robust if it agrees on 7-8 years, and  
 846 transitional if on 6 or fewer years.



847 **Table 1.** Simulations with different scenarios evaluated by INLAND model in Amazonia-Cerrado  
 848 transition. CA, climatological average, 1961-1990; CV, monthly climate data, 1948-2008; the nutrient  
 849 limitation on  $V_{\max}$  - PC, no phosphorus limitation ( $V_{\max} = 65 \mu\text{molCO}_2 \text{ m}^{-2} \text{ s}^{-1}$ ); PR, regional phosphorus  
 850 limitation; PG, global phosphorus limitation).

Climate	CO <sub>2</sub>	Fire (F)	$V_{\max}$		
			PC	PR	PG
CA	Variable	Off	CA+PC	CA+PR	CA+PG
CA	Variable	On	CA+PC+F	CA+PR+F	CA+PG+F
CV	Variable	Off	CV+PC	CV+PR	CV+PG
CV	Variable	On	CV+PC+F	CV+PR+F	CV+PG+F

851

852

853 **Table 2.** Individual and combined effects for each simulation in Amazonia-Cerrado transition. CA,  
 854 climatological seasonal average, 1961-1990; CV, monthly climate data, 1948-2008; the nutrient limitation  
 855 on  $V_{\max}$  - PC, no phosphorus limitation ( $V_{\max} = 65 \mu\text{molCO}_2 \text{ m}^{-2} \text{ s}^{-1}$ ); PR, regional phosphorus limitation;  
 856 PG, global phosphorus limitation)

Climate (C)	Phosphorus (P)	Fire (F)
(CV+PC)-(CA+PC)	(CA+PR)-(CA+PC)	(CA+PC+F)-(CA+PC)
(CV+PR)-(CA+PR)	(CV+PR)-(CV+PC)	(CV+PC+F)-(CV+PC)
(CV+PG)-(CA+PG)	(CA+PG)-(CA+PC)	(CA+PR+F)-(CA+PR)
	(CV+PG)-(CV+PC)	(CV+PR+F)-(CV+PR)
		(CA+PG+F)-(CA+PG)
		(CV+PG+F)-(CV+PG)

857

858





859 **Table 3.** Summary of average NPP, LAI and AGB for the Amazonia-Cerrado transition at the  
 860 transects domains, considering all simulations with CA and CV regardless of fire presence or phosphorus  
 861 limitation. The results of a one-way ANOVA are also shown, including the  $F$  statistic, and  $p$  value. Values  
 862 within each column followed by a different letter are significantly different ( $p < 0.05$ ) according to the  
 863 Tukey–Kramer test.

Group 1	NPP		LAI <sub>total</sub>		LAI <sub>lower</sub>		LAI <sub>upper</sub>		AGB	
	kg-C m <sup>-2</sup> yr <sup>-1</sup>		m <sup>2</sup> m <sup>-2</sup>		m <sup>2</sup> m <sup>-2</sup>		m <sup>2</sup> m <sup>-2</sup>		kg-C m <sup>-2</sup>	
CA	0.68	a	7.47	a	1.98	a	5.49	a	6.68	a
CV	0.64	b	7.15	b	2.11	a	5.04	b	6.30	b
$F$	40.2		57.2		2.96		36.0		11.3	
$p$	<0.001		<0.001		<i>ns</i>		<0.01		<0.001	

864

865 **Table 4.** Summary of average NPP, LAI and AGB for the transition at the transects domains, considering  
 866 different phosphorus limitation, regardless of climate and fire presence. The results of a one-way ANOVA  
 867 are also shown, including the  $F$  statistic, and  $p$  value. Values within each column followed by a different  
 868 letter are significantly different ( $p < 0.05$ ) according to the Tukey–Kramer test.

Group 2	NPP		LAI <sub>total</sub>		LAI <sub>lower</sub>		LAI <sub>upper</sub>		AGB	
	kg-C m <sup>-2</sup> yr <sup>-1</sup>		m <sup>2</sup> m <sup>-2</sup>		m <sup>2</sup> m <sup>-2</sup>		m <sup>2</sup> m <sup>-2</sup>		kg-C m <sup>-2</sup>	
PC	0.71	a	7.64	a	1.84	b	5.80	a	7.15	a
PR	0.64	b	7.15	b	2.19	a	4.95	b	6.20	b
PG	0.64	b	7.14	b	2.10	a	5.04	b	6.12	b
$F_{2,99}$	62.8		61.0		8.75		53.5		33.6	
$p$	<0.001		<0.001		<0.01		<0.01		<0.001	

869

870



871 **Table 5.** Summary of average NPP, LAI and biomass for the transition at the transects domains,  
 872 considering presence or absence of fire. The results of a one-way ANOVA are also shown, including the  
 873 *F* statistic, and *p* value. Values within each column followed by a different letter are significantly different  
 874 ( $p < 0.05$ ) according to the Tukey–Kramer test.

Group 3	NPP		LAI <sub>total</sub>		LAI <sub>lower</sub>		LAI <sub>upper</sub>		AGB	
	kg-C m <sup>-2</sup> yr <sup>-1</sup>		m <sup>2</sup> m <sup>-2</sup>		m <sup>2</sup> m <sup>-2</sup>		m <sup>2</sup> m <sup>-2</sup>		kg-C m <sup>-2</sup>	
Fire OFF	0.66	a	6.72	b	0.88	b	5.84	a	8.47	b
Fire ON	0.67	b	7.90	a	3.21	a	4.69	b	4.51	a
<i>F</i> <sub>3,84</sub>	8.28		937		1459		249		1719	
<i>p</i>	<0.005		<0.001		<0.01		<0.01		<0.001	

875

876



877 **Table 6.** Summary of average NPP, LAI and AGB for the transition at the transects domains, considering  
 878 all factor combinations. The results of a one-way ANOVA are also shown, including the  $F$  statistic, and  
 879  $p$  value. Values within each column followed by a different letter are significantly different ( $p < 0.05$ )  
 880 according to the Tukey–Kramer test.

	<b>NPP</b>		<b>LAI<sub>total</sub></b>		<b>LAI<sub>lower</sub></b>		<b>LAI<sub>upper</sub></b>		<b>AGB</b>	
	kg-C m <sup>-2</sup> yr <sup>-1</sup>		m <sup>2</sup> m <sup>-2</sup>		m <sup>2</sup> m <sup>-2</sup>		m <sup>2</sup> m <sup>-2</sup>		kg-C m <sup>-2</sup>	
CV+PC	0.69	bcd	6.96	d	0.84	e	6.48	a	9.01	ab
CV+PG	0.61	f	6.24	f	0.85	e	5.60	bc	7.91	c
CV+PR	0.62	f	6.33	f	0.85	e	5.74	bc	8.04	c
CV+PC+F	0.69	abc	7.92	b	2.91	cd	4.61	ef	4.89	de
CV+PG+F	0.63	ef	7.76	b	3.73	a	5.81	bc	3.91	f
CV+PR+F	0.63	ef	7.65	bc	3.47	ab	4.69	ef	4.02	f
CA+PC	0.72	ab	7.39	c	0.91	e	6.12	ab	9.31	a
CA+PG	0.64	def	6.64	e	0.91	e	5.40	cd	8.22	c
CA+PR	0.65	cdef	6.72	de	0.91	e	5.49	cd	8.31	bc
CA+PC+F	0.74	a	8.29	a	2.69	d	5.02	de	5.40	d
CA+PG+F	0.67	cde	7.90	b	3.29	abc	4.04	g	4.45	ef
CA+PR+F	0.67	cde	7.88	b	3.19	bc	4.18	fg	4.42	ef
$F$	16.2		115		140		38.1		172	
$p$	<0.001		<0.001		<0.01		<0.01		<0.001	

881

882

883 **Table 7.** Correlation coefficients of biomass simulated by INLAND and field estimates

	<b>T1</b>	<b>T2</b>	<b>T3</b>	<b>T4</b>	<b>T5</b>	<b>All transects</b>
CA+PC	0.843	0.928	0.886	0.937	0.337	0.786
CV+PC	0.838	0.884	0.890	0.939	0.355	0.781
CA+PR	0.793	0.848	0.830	0.911	0.399	0.756
CV+PR	0.795	0.793	0.832	0.907	0.527	0.771
CA+PG	0.814	0.951	0.838	0.889	0.388	0.776
CV+PG	0.825	0.922	0.840	0.879	0.496	0.792
CA+PC+F	0.988	0.987	0.977	0.892	0.133	0.795
CV+PC+F	0.976	0.947	0.933	0.908	0.187	0.790
CA+PR+F	0.842	0.805	0.981	0.808	0.561	0.799
CV+PR+F	0.925	0.804	0.927	0.808	0.319	0.757
CA+PG+F	0.844	0.961	0.980	0.830	0.430	0.809
CV+PG+F	0.845	0.932	0.931	0.881	0.177	0.753
CA avg	0.854	0.913	0.915	0.878	0.375	0.787
CV avg	0.867	0.880	0.892	0.887	0.344	0.774

884

885

886